


PRIMARY RESEARCH

Open Access



# Arachidonic acid-induced $\text{Ca}^{2+}$ entry and migration in a neuroendocrine cancer cell line

Priyodarshan Goswamee, Tamar Pounardjian and David R. Giovannucci\* 

## Abstract

**Background:** Store-operated  $\text{Ca}^{2+}$  entry (SOCE) has been implicated in the migration of some cancer cell lines. The canonical SOCE is defined as the  $\text{Ca}^{2+}$  entry that occurs in response to near-maximal depletion of  $\text{Ca}^{2+}$  within the endoplasmic reticulum. Alternatively, arachidonic acid (AA) has been shown to induce  $\text{Ca}^{2+}$  entry in a store-independent manner through Orai1/Orai3 hetero-multimeric channels. However, the role of this AA-induced  $\text{Ca}^{2+}$  entry pathway in cancer cell migration has not been adequately assessed.

**Methods:** The present study investigated the involvement of AA-induced  $\text{Ca}^{2+}$  entry in migration in BON cells, a model gastro-enteropancreatic neuroendocrine tumor (GEPNET) cell line using pharmacological and gene knock-down methods in combination with live cell fluorescence imaging and standard migration assays.

**Results:** We showed that both the store-dependent and AA-induced  $\text{Ca}^{2+}$  entry modes could be selectively activated and that exogenous administration of AA resulted in  $\text{Ca}^{2+}$  entry that was pharmacologically distinct from SOCE. Also, whereas homomeric Orai1-containing channels appeared to largely underlie SOCE, the AA-induced  $\text{Ca}^{2+}$  entry channel required the expression of Orai3 as well as Orai1. Moreover, we showed that AA treatment enhanced the migration of BON cells and that this migration could be abrogated by selective inhibition of the AA-induced  $\text{Ca}^{2+}$  entry.

**Conclusions:** Taken together, these data revealed that an alternative Orai3-dependent  $\text{Ca}^{2+}$  entry pathway is an important signal for GEPNET cell migration.

**Keywords:** Orai, Arachidonic acid, Calcium signaling, Calcium channels, Cell migration, Neuroendocrinology, Gastro-enteropancreatic neuroendocrine tumors

## Background

In the last decade, Orai1 and stromal interacting molecule-1 (STIM1) were identified as the long sought-after molecular players that are both necessary and sufficient to recapitulate store-operated  $\text{Ca}^{2+}$  entry (SOCE) [1–8]. This pathway was shown to be physiologically and pathophysiologically important for a variety of cell types including, lymphocytes and cancer cells [9–11]. Recently, several studies have indicated a role for Orai1 and STIM1 in migration of different types of cancer and non-cancer

cells [12–21]. These observations have led to the consensus that SOCE is important for tumor cell migration [22]. Interestingly, alternative pathways that utilize many of the same molecular constituents of SOCE have been shown to contribute to other less well-characterized modes of  $\text{Ca}^{2+}$  entry [23, 24]. However, these alternative pathways have not been adequately investigated in the context of tumor cell migration. For example, the intracellular lipid second messenger, arachidonic acid (AA) and/or its downstream metabolite leukotriene-C4 (LTC4) have been shown to induce a store-independent mode of  $\text{Ca}^{2+}$  entry via a plasma-membrane channel that is comprised of both Orai1 and Orai3 [14, 25].

\*Correspondence: david.giovannucci@utoledo.edu  
Department of Neurosciences, University of Toledo Medical Center, 3000  
Arlington Avenue, Toledo, OH 43614-2598, USA

Although some studies indicated that AA or its metabolites such as prostaglandins and leukotrienes might stimulate migration and epithelial to mesenchymal transition (EMT) in some cancer and non-cancer cells [26–29], a role for AA-induced  $\text{Ca}^{2+}$  entry has not been examined. Therefore, we ascertained whether SOCE and/or AA-induced  $\text{Ca}^{2+}$  entry pathways contributed to cell migration in a tumor-cell line that displayed both pathways.

Previous research from our laboratory had shown that several model cell lines of gastroenteropancreatic neuroendocrine tumors (GEPNETs) expressed mRNA message for Orai homologs and exhibited SOCE [30]. In the current study, we extended these observations to assess whether exogenously administered AA could evoke  $\text{Ca}^{2+}$  entry and/or enhancement of cell migration in BON cells, a well-characterized GEPNET cell line.

Using live cell fluorimetric imaging of  $\text{Ca}^{2+}$  dynamics in combination with pharmacological treatments, we demonstrated that  $\text{Ca}^{2+}$  entry in this cell type could be induced by artificially depleting the ER stores or by exogenous application of AA. We also demonstrated that these modes of  $\text{Ca}^{2+}$  entry could be evoked and perturbed selectively. We identified the Orai channels that contributed to these two  $\text{Ca}^{2+}$  entry pathways using shRNA-mediated gene knockdown. These studies revealed that expression of Orai1 was required for SOCE and that the AA-induced pathway required both Orai1 and Orai3. Furthermore, we assessed the relative roles of SOCE and AA-induced  $\text{Ca}^{2+}$  entry in BON cell migration using a modified Boyden chamber assay. Selective stimulation or perturbation of these  $\text{Ca}^{2+}$  entry modes using a variety of pharmacological and molecular tools revealed that under our experimental conditions the AA-induced  $\text{Ca}^{2+}$  entry was the dominant  $\text{Ca}^{2+}$ -signal responsible for BON cell migration. Our results suggest that  $\text{Ca}^{2+}$  entry through an Orai3-containing channel is a novel signal for BON cell migration and identifies this pathway as a potential target to limit recurring GEPNET metastasis.

## Methods

### Materials

Cyclopiazonic acid (CPA) was purchased from Calbiochem. Arachidonic acid was obtained from MP Biochemicals. Thapsigargin and SK&F 96365 (SKF) were purchased from Tocris Bioscience. Ketoprofen, ethylene glycol tetraacetic acid (EGTA) and 2-aminoethoxydiphenyl borate (2-APB) were obtained from Sigma. Leukotriene  $\text{C}_4$  (LTC<sub>4</sub>) and Nordihydroguaiaretic acid (NDGA) were purchased from Cayman chemical.

### Cell culture and transfection

BON cells were cultured in flasks with a 1:1 solution of DMEM and F12K supplemented with 10% fetal bovine serum (FBS) and 1% penicillin–streptomycin and maintained at 37 °C in a humidified incubator with 5%  $\text{CO}_2$ . All cell culture reagents were obtained from Life Technologies, unless specifically indicated. For cell transfection,  $5 \times 10^6$  BON cells were electroporated with plasmid vectors containing shRNAs against Orai1 or Orai3 (Origene Technologies) using the Amaxa nucleofector II device (Lonza) as per manufacturer's instruction. All available shRNA constructs supplied by the manufacturer resulted in comparable knockdowns for each subunit, and the data from these experiments were pooled. Transfection efficiency was estimated to be approximately 90% for both constructs. Control cells were transfected with an identical plasmid that contained a scrambled message. Moreover, mock-transfected and untransfected cells were used as additional controls. All plasmids expressed either GFP or RFP and a gene for puromycin resistance. Transfected cells were maintained 2 days in culture medium containing 0.2  $\mu\text{g}/\text{ml}$  puromycin dihydrochloride. In addition to western blotting (see below), knockdown of Orai1 and 3 were functionally verified using live cell  $\text{Ca}^{2+}$  imaging at different time points and the maximum effects were observed at 48 h after transfection.

### Western blotting

Lysates were prepared from BON cells at 48 h post-transfection by extraction of cellular proteins in RIPA buffer (containing 25 mM Tris–HCl, pH 7.6, 150 mM NaCl, 1% Triton X-100, 1% sodium deoxycholate, 0.1% SDS). The cell lysates were concentrated and desalted using the YM-100 Microcon centrifuge filter (Sigma Aldrich). Approximately, 50  $\mu\text{g}$  of concentrated cell lysates were run on 8% Bis–Tris gels under denaturing conditions. Following separation, the protein bands were transferred onto polyvinylidene fluoride (PVDF) membranes for 90 min using the Criterion blotter (Biorad) under semi-wet conditions. The membranes were then incubated for 2 h in a solution of 5% non-fat dry milk in TBS-T buffer (containing in mM, 20 Tris/HCl, 150 NaCl and 0.1% Tween-20) to block non-specific interactions. The membranes were then cut in two and incubated overnight at 4°C with rabbit polyclonal antisera against Orai1 or Orai3 (Prosci). The membranes were washed with TBS-T buffer and probed for 2 h using an HRP-conjugated anti-rabbit secondary antibody (Millipore). Finally, the blots were washed with TBS-T buffer and treated for chemiluminescence visualization using the ECL Western Blotting substrate (Pierce). Detection of protein bands was performed using a LAS 3000 imaging system (Fujifilm). After matching the position of the bands of interests

with respect to the molecular mass reference ladder (Invitrogen), the membranes were stripped using Restore solution, (Pierce) and re-probed with HRP-conjugated mouse monoclonal antibody against  $\beta$ -actin (Abcam) and visualized by chemiluminescence. Quantification of band density was achieved using NIH ImageJ software. The intensity of bands for Orai1 and Orai3 were comparable in untransfected, mock transfected and scrambled shRNA-transfected BON cells.

#### Live cell imaging

Changes in cytosolic  $\text{Ca}^{2+}$  levels in live cells were performed using live-cell fluorescent imaging as described previously [30]. Briefly, BON cells cultured on glass coverslips were loaded with a 2  $\mu\text{M}$  fura-2 AM solution prepared in a physiological saline (containing in mM 140 NaCl, 5 KCl, 2.2  $\text{CaCl}_2$ , 1  $\text{MgCl}_2$ , 10 HEPES, and 5 glucose, pH 7.4) for 30–40 min at room temperature. Changes in intracellular  $\text{Ca}^{2+}$  were represented as the ratio of fura-2 fluorescence at 510 nm evoked by sequential excitation at 340 and 380 nm at a frequency of 1 Hz. Typically, for live cell imaging experiments changes in  $\text{Ca}^{2+}$  for 20–40 cells were independently monitored and analyzed. For each experiment, 2–3 coverslips were analyzed and averaged results from at least three independent experiments were used to perform statistical analysis.

#### $\text{Mn}^{2+}$ quench assay

Rate of  $\text{Ca}^{2+}$  entry independent of  $\text{Ca}^{2+}$  release or buffering was estimated by monitoring the rate of quenching of the fura-2 fluorescence signal excited at 360 nm in response to  $\text{Mn}^{2+}$  entry as previously described [30]. The rate of  $\text{Mn}^{2+}$  quench of the fura-2 fluorescence in response to pharmacological stimulation was compared with the basal rate under the unstimulated condition. The fold change in the rates of quenching from basal values was determined.

#### Migration assay

BON cell migration was assessed as described previously using a modified Boyden chamber assay [31]. Briefly,  $5.0 \times 10^4$  BON cells were re-suspended in serum free media (SFM) and were seeded into the upper chamber, the bottom surfaces of which were coated with 50  $\mu\text{g}/\text{ml}$  Type-1 rat-tail collagen (Corning Incorporated). The lower chamber was loaded with SFM containing AA with or without pharmacological inhibitors. In some experiments, the cells were pre-treated with 1  $\mu\text{M}$  thapsigargin dissolved in  $\text{Ca}^{2+}$ -free SFM for 15 min. In another experiment, the concentration of free  $\text{Ca}^{2+}$  was reduced to approximately 0.7 mM by adding EGTA to the media. The cells were allowed to migrate from the upper to lower chamber for 8–12 h. Following this time-period the

number of migrated cells were counted and expressed as percentage of the total number seeded.

#### Immunofluorescence

Immunofluorescence was used to identify various NMT markers in BON cells prior to or following arachidonic acid treatments. BON cells ( $5 \times 10^4$  cells) were seeded onto glass coverslips or Boyden chamber inserts placed in a 6-well dish containing growth media. Following treatments, cells were fixed using a 4% paraformaldehyde solution and washed with phosphate buffered saline (PBS) (Life tech). Cells were then permeabilized using a 0.5% Triton X-100 solution (Sigma) for 5 min at and a blocking buffer containing 5% non-fat dry milk added for 1 h. Following PBS washes, samples were incubated overnight at 4 °C with the appropriate primary antibody in a humidified chamber. After PBS washes, glass coverslips were incubated with secondary antibodies conjugated to Alexa Fluor 488 or Alexa Fluor 546 for 1 h and mounted with Vectashield antifade medium (Vector Laboratories). F-actin was labeled using phallotoxin conjugated to Alexa Fluor 546 or 633. Images were obtained using a Leica SP5 Confocal microscope.

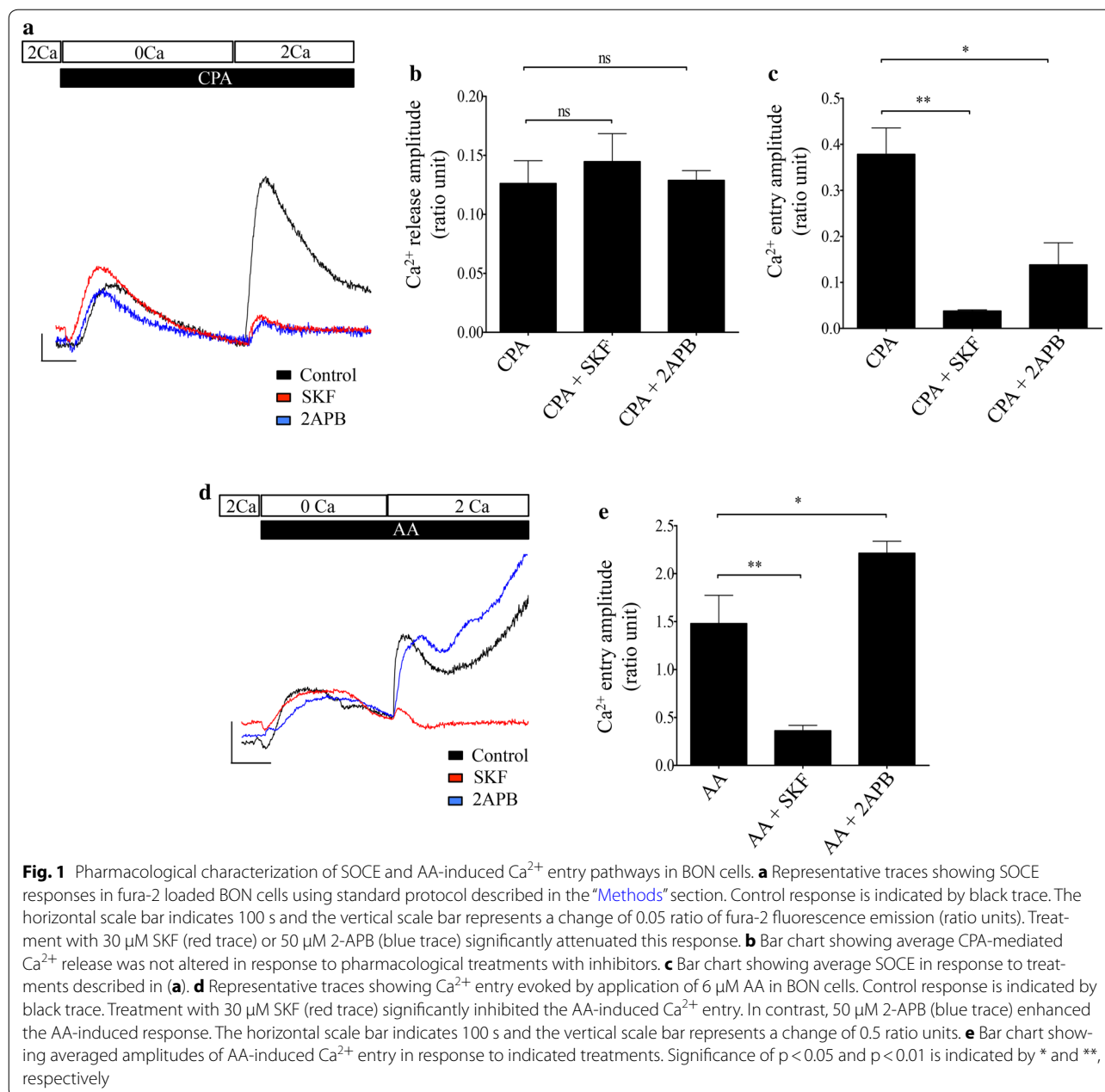
#### Statistical analyses

The results from the live cell imaging and  $\text{Mn}^{2+}$ -quench, were analyzed using one-way analysis of variance (ANOVA) and Dunnett's tests were performed to assess significance among treatment groups. BON cell migration experiments using genetic and pharmacological manipulations were assessed by Tukey's multiple comparison tests. The statistical significance of the western blot data was analyzed by 2-tailed t tests.

## Results

#### Store-operated and AA induced $\text{Ca}^{2+}$ entry are pharmacologically distinguishable in BON cells

An initial set of experiments was performed to pharmacologically characterize store-operated and arachidonic acid (AA)-activated forms of  $\text{Ca}^{2+}$  entry in BON cells by selective blockade using a broadly selective  $\text{Ca}^{2+}$  channel blocker SK&F 96365 (SKF) or 2-aminoethoxydiphenyl borate (2-APB) that has been shown to be less effective at blocking Orai3-containing  $\text{Ca}^{2+}$  channels. Store-operated  $\text{Ca}^{2+}$  entry (SOCE) was assessed using a standard protocol to deplete the endoplasmic reticulum (ER) stores of  $\text{Ca}^{2+}$  by treatment with 30  $\mu\text{M}$  cyclopiazonic acid (CPA), a reversible inhibitor of the sarco-endoplasmic reticulum  $\text{Ca}^{2+}$ -ATPase (SERCA). The CPA was dissolved in a saline containing nominal  $\text{Ca}^{2+}$  (0.5 mM EGTA with no added  $\text{Ca}^{2+}$ ). As shown in Fig. 1a, following CPA treatment there was a transient increase in concentration of cytoplasmic  $\text{Ca}^{2+}$  ( $[\text{Ca}^{2+}]_{\text{cyt}}$ ) that indicated depletion of



$\text{Ca}^{2+}$  from the ER ( $[\text{Ca}^{2+}]_{ER}$ ). Following restoration of 2.2 mM  $\text{Ca}^{2+}$  to the bath solution, a second, larger transient elevation in  $[\text{Ca}^{2+}]_{cyt}$  was observed indicative of SOCE. As shown in Fig. 1a, c, activation of SOCE using standard protocol resulted in a change of  $0.38 \pm 0.05$  ratio units ( $n=3$ ), whereas, treatment with 30  $\mu\text{M}$  SKF ( $n=3$ ) or 50  $\mu\text{M}$  2-APB ( $n=3$ ) greatly attenuated the SOCE responses. The mean peak amplitudes of the response in SKF- or 2-APB-treated cells were  $0.04 \pm 0.00$  and  $0.14 \pm 0.05$  ratio units, respectively ( $n=3$ ). As shown in Fig. 1b, treatment with SKF or 2-APB did not have a significant effect on the store-content, as reflected by the

CPA-mediated  $\text{Ca}^{2+}$  release. While, the average amplitude of the CPA-mediated release in control cells was  $0.13 \pm 0.02$  ratio units, treatment with SKF and 2-APB resulted in  $\text{Ca}^{2+}$  release with the average amplitudes of  $0.14 \pm 0.02$  and  $0.13 \pm 0.01$  ratio units, respectively.

We next tested whether addition of AA activated a distinct  $\text{Ca}^{2+}$  entry pathway. Application of exogenous 1–30  $\mu\text{M}$  AA induced elevations in  $[\text{Ca}^{2+}]_{cyt}$  in a concentration-dependent manner (Additional file 1: Figure S1). A sub-maximal dose of 6  $\mu\text{M}$  AA was used to treat cells for all the experiments described in the current study. As shown in Fig. 1d, application of 6  $\mu\text{M}$  AA in

nominal  $\text{Ca}^{2+}$ -containing bath solution induced an initial transient rise in  $[\text{Ca}^{2+}]_{\text{cyt}}$  that was followed by robust sustained elevation in  $[\text{Ca}^{2+}]_{\text{cyt}}$  following return of  $\text{Ca}^{2+}$  in the bath solution. Typically, the secondary responses were complex waveforms and we used the peak amplitude measured within the first 300 s post-application as an index of the magnitude of the AA-induced  $\text{Ca}^{2+}$  entry. On average in about 60% of the cells, treatment with AA resulted in  $\text{Ca}^{2+}$  response with bimodal kinetics, while the other 40% of cells responded with a gradual rise and sustained increase in  $[\text{Ca}^{2+}]_{\text{cyt}}$ . These responses were in contrast to those evoked by SOCE that showed only a transient rise in cytosolic calcium. It was unclear as to what underlies the difference between these populations. Examples of these AA-induced responses are shown in Additional file 1: Figure S1. The average change in amplitude for all the experiment was  $1.48 \pm 0.29$  ratio units ( $n=3$ ). To further distinguish AA-induced  $\text{Ca}^{2+}$  entry from SOCE we assessed the effects of known pharmacological inhibitors of SOCE. As shown in Fig. 1d, e, the AA-induced rise in  $[\text{Ca}^{2+}]_{\text{cyt}}$  was substantially diminished by 30  $\mu\text{M}$  SKF with average change in amplitude of  $0.36 \pm 0.06$  ratio units ( $n=4$ ). In contrast, the AA-induced rise in  $[\text{Ca}^{2+}]_{\text{cyt}}$  was not diminished by treatment with 50  $\mu\text{M}$  2-APB and was  $2.21 \pm 0.12$  ratio units ( $n=3$ ), demonstrating that the SOCE and the AA-induced  $\text{Ca}^{2+}$  entry pathways were pharmacologically distinguishable.

We next performed a series of manganese quench assays to measure the rates of quenching and follow divalent ion entry independent of potential contribution by  $\text{Ca}^{2+}$  buffering, clearance or release from internal stores. The rates of the  $\text{Mn}^{2+}$ -induced quench of the fluorescence response following activation or inhibition of SOCE and the AA-induced responses was determined and compared against the rate of quenching in unstimulated cells. As shown in Fig. 2a, b, CPA-induced store depletion resulted in a nearly sixfold faster rate of quenching than that measured in unstimulated cells. The normalized rate of quenching for unstimulated cells was  $1.00 \pm 0.10$  fluorescent unit (FU)/s ( $n=4$ ), whereas that after CPA treatment was  $5.56 \pm 0.87$  FU/s ( $n=4$ ). Treatment with both SKF, as well as, 2-APB diminished the rate of quenching compared to the unstimulated cells to  $0.94 \pm 0.50$  FU/s ( $n=3$ ) and  $0.58 \pm 0.37$  FU/s ( $n=4$ ), respectively. Treatment with 30  $\mu\text{M}$  SKF or 50  $\mu\text{M}$  2-APB alone had no effect on the unstimulated rate of entry (data not shown). Consistent with the activation of a  $\text{Ca}^{2+}$  entry channel, treatment with AA resulted in rapid quenching of the fura-2 fluorescence signal. In this case the rate of quenching was  $14.36 \pm 0.59$  FU/s ( $n=4$ ), indicating that the rate of entry was approximately 2.5 fold faster than the CPA-evoked rate of entry, and 14 times faster than the unstimulated rate of entry. In contrast to the CPA-treated cells, 2-APB

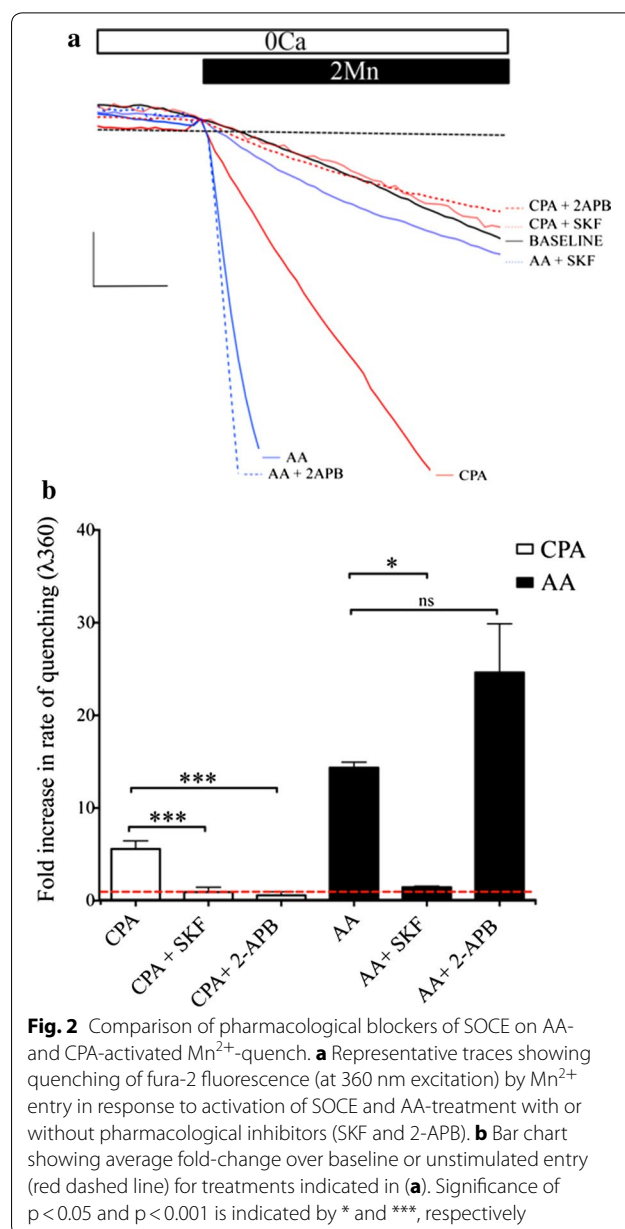


**Fig. 2** Comparison of pharmacological blockers of SOCE on AA- and CPA-activated  $\text{Mn}^{2+}$ -quench. **a** Representative traces showing quenching of fura-2 fluorescence (at 360 nm excitation) by  $\text{Mn}^{2+}$  entry in response to activation of SOCE and AA-treatment with or without pharmacological inhibitors (SKF and 2-APB). **b** Bar chart showing average fold-change over baseline or unstimulated entry (red dashed line) for treatments indicated in (a). Significance of  $p < 0.05$  and  $p < 0.001$  is indicated by \* and \*\*\*, respectively

treatment had no significant effect on the rate of AA-induced entry, and the rate of quenching was  $24.62 \pm 5.26$  FU/s ( $n=4$ ). Treatment with SKF however, resulted in significant diminishment of entry. The normalized rate of AA-induced quenching was reduced to  $1.45 \pm 0.12$  FU/s ( $n=4$ ) by treatment with SKF.

#### Arachidonic acid induced $\text{Ca}^{2+}$ release from ER but did not activate SOCE

As shown in Fig. 1d, treatment with AA induced a rise in  $[\text{Ca}^{2+}]_{\text{cyt}}$  in the absence of extracellular  $\text{Ca}^{2+}$ . Therefore, we asked if the rise in  $[\text{Ca}^{2+}]_{\text{cyt}}$  resulted from ER  $\text{Ca}^{2+}$  release and whether this release was sufficient to depleted

the  $[Ca^{2+}]_{ER}$  and trigger SOCE. To determine whether AA-induced  $Ca^{2+}$  release from the ER, we pre-treated the cells in nominal  $Ca^{2+}$  containing saline with thapsigargin (TSG), an irreversible inhibitor of the SERCA pump, and then applied AA. As shown in Fig. 3a (upper panel), 1  $\mu$ M TSG induced robust, transient release of  $Ca^{2+}$  from ER stores. Subsequent application of AA did not induce significant additional release. The mean amplitude of this signal was only  $0.007 \pm 0.001$  ratio units ( $n=4$ ). In contrast, in time-matched control experiments (lower panel), where TSG treatment was omitted, AA evoked  $Ca^{2+}$  release with mean amplitude of  $0.24 \pm 0.05$  ratio units ( $n=4$ ), a value similar in magnitude to TSG-evoked release. These results indicated that AA mobilized  $Ca^{2+}$  release from a TSG- or CPA-sensitive intracellular store of  $Ca^{2+}$ . Thus, to test whether AA treatment depleted

$[Ca^{2+}]_{ER}$ , a signal that is necessary to trigger canonical SOCE, we reversed the sequence of treatment as shown in Fig. 3b (upper panel). When AA was applied first, the  $[Ca^{2+}]_{cyt}$  gradually increased to a new steady state about 200 s. Subsequent addition of TSG resulted in an additional release of  $Ca^{2+}$  with mean amplitude of  $0.08 \pm 0.01$  ratio units ( $n=3$ ). However, this  $Ca^{2+}$  release signal was significantly smaller than that evoked by TSG alone (on average  $0.19 \pm 0.03$  ratio units ( $n=3$ ) as shown in a time-matched control experiment (Fig. 3b: lower panel). This demonstrated that AA mobilized  $[Ca^{2+}]_{ER}$  but did not deplete the ER in our experimental paradigm. Moreover, mobilization of  $[Ca^{2+}]_{ER}$  by treatment with AA was not sufficient to trigger SOCE (Fig. 3d, upper panel). As shown in Fig. 3d, e, following restoration of  $Ca^{2+}$  in the bath, the mean change in amplitude for cells that were

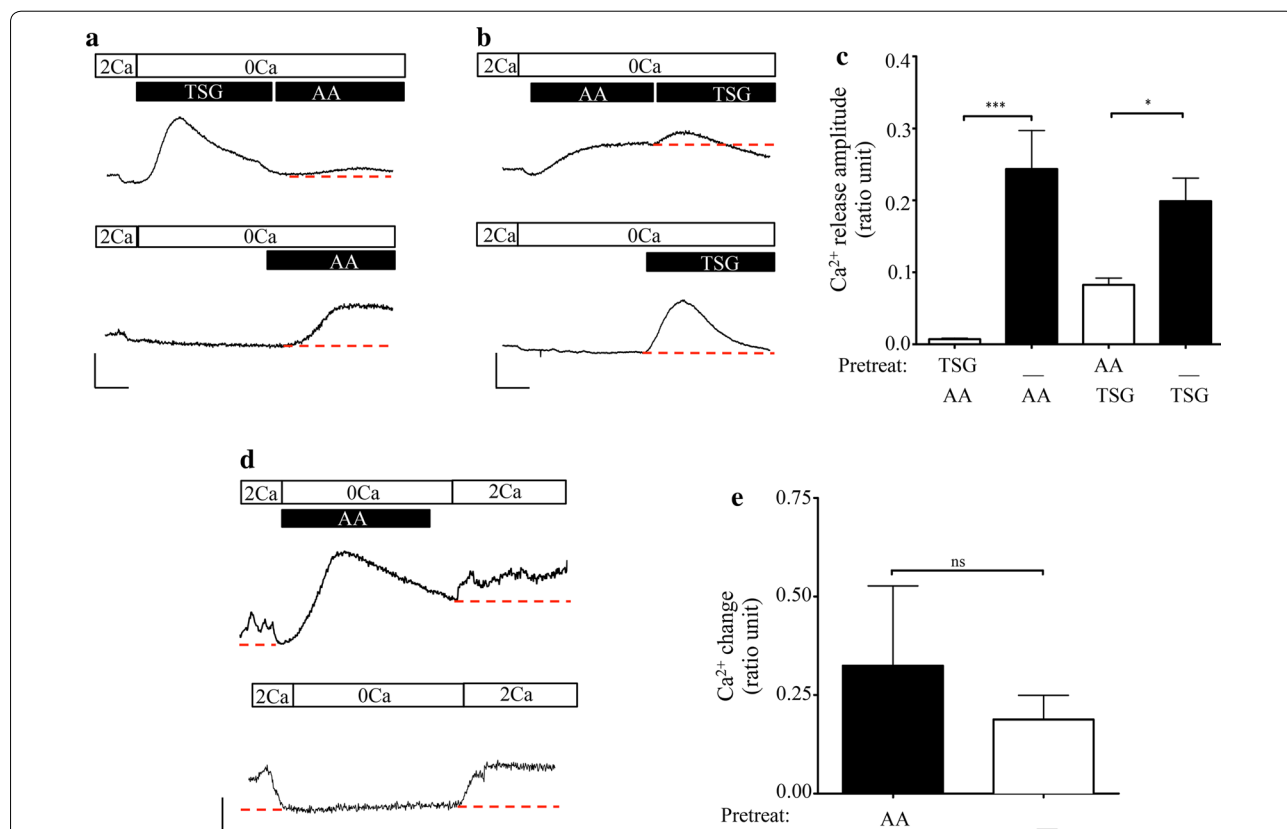


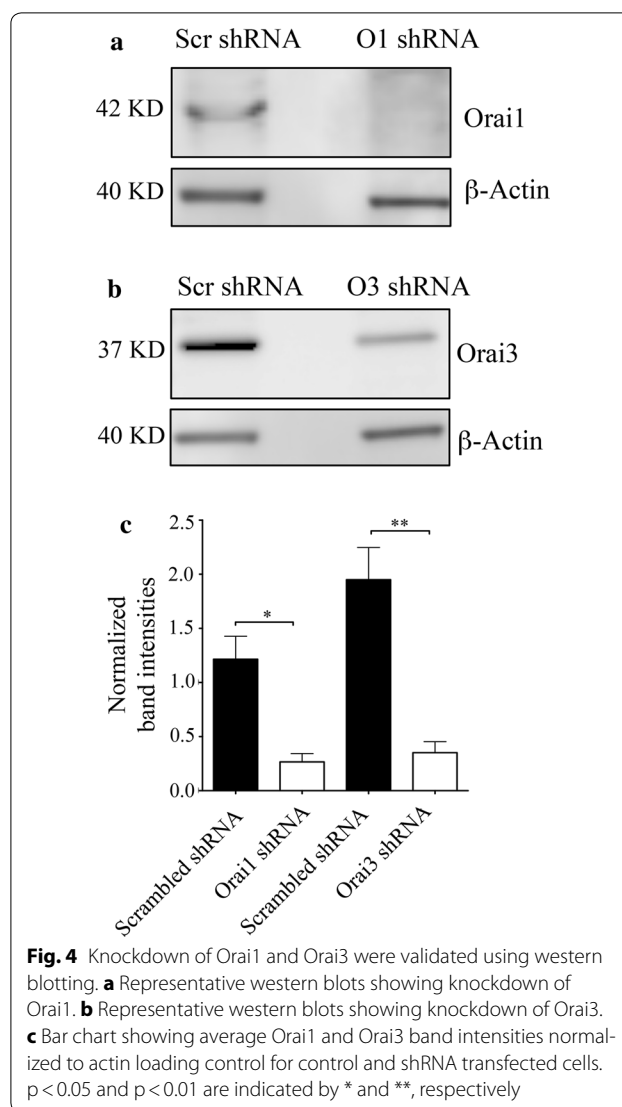
**Fig. 3** Treatment with AA depleted  $[Ca^{2+}]_{ER}$ , but was not sufficient to evoke SOCE. **a** Upper panel: representative trace showing pre-treatment of fura-loaded BON cells with 1  $\mu$ M TSG in nominal  $Ca^{2+}$ -containing media abolished AA-mediated release. Lower panel: representative time-matched control trace where TSG pre-treatment was omitted. Scale bars indicate 100 s (horizontal) and 0.1 ratio units (vertical). **b** Upper panel: representative trace showing pre-treatment with 6  $\mu$ M AA in nominal  $Ca^{2+}$ -containing media significantly diminished the TSG-mediated release. Lower panel: representative time-matched control trace where pre-treatment with AA was omitted. Scale bars indicate 100 s and 0.1 ratio units. **c** Bar chart showing average data for treatments indicated in panels **a** and **b**. **d** Upper panel: representative trace showing the effect of pre-treatment with 6  $\mu$ M AA in nominal  $Ca^{2+}$ -containing media on  $Ca^{2+}$  entry. Lower panel: representative time-matched control trace where pre-treatment with AA was omitted. Scale bars: x-axis = 100 s, y-axis = 0.1 ratio units. **e** Bar chart showing average change in cytosolic  $Ca^{2+}$  levels in response to change in extracellular  $Ca^{2+}$  concentration. In figures **a**, **b** and **d** magnitude of  $Ca^{2+}$  responses were measured by determining change in amplitude with respect to the red dashed line. Significance of  $p < 0.05$  and  $p < 0.001$  is indicated by \* and \*\*\*, respectively

pre-treated with AA in nominal  $\text{Ca}^{2+}$ -containing solution was  $0.32 \pm 0.20$  ratio units ( $n=3$ ) (Fig. 3d, upper panel). If pre-treatment with AA was omitted, the mean change in the signal amplitude was  $0.19 \pm 0.06$  ratio units ( $n=3$ ). These slight changes in ratio values reflected the change in steady state between  $\text{Ca}^{2+}$ -containing and  $\text{Ca}^{2+}$ -free media and indicated that (1) AA-induced mobilization of  $[\text{Ca}^{2+}]_{ER}$  did not activate  $\text{Ca}^{2+}$  entry and (2) that continuous presence of AA was needed to sustain AA-induced  $\text{Ca}^{2+}$  entry.

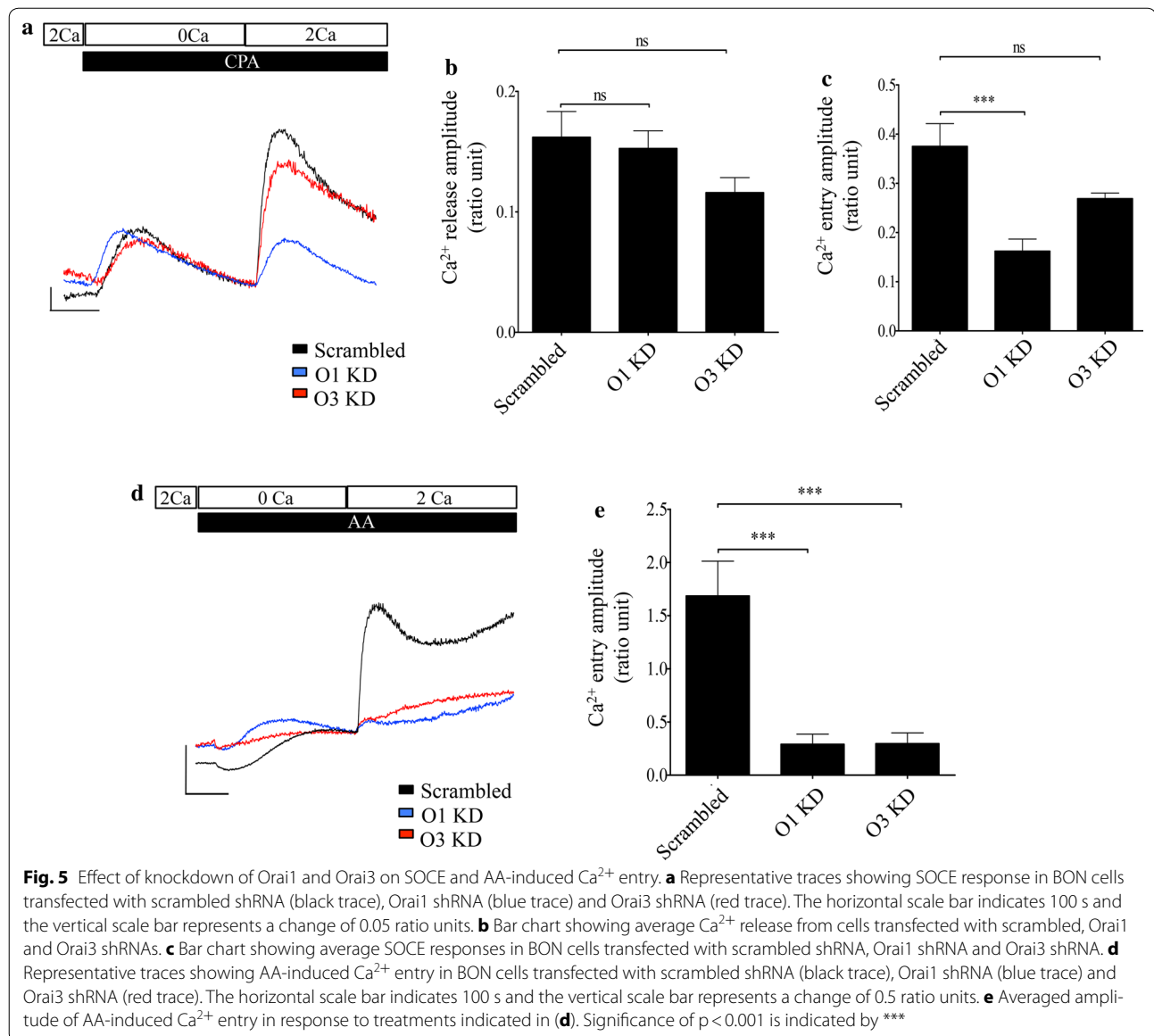
#### Contribution of Orai1 and Orai3 to store operated and AA-induced $\text{Ca}^{2+}$ entry

Because SOCE and the AA-induced  $\text{Ca}^{2+}$  entry pathways could be distinguished functionally in BON cells, we investigated the requirements of Orai1 and Orai3 channel subunits for these modes of  $\text{Ca}^{2+}$  entry. Specific channel subunits in BON cells were selectively knocked down by transfecting with plasmids that expressed short hairpin RNAs (shRNAs) for Orai1, Orai3 and scrambled sequences for either genes of interest as controls. Since, previous work indicated that BON cells express low levels of Orai2 mRNA, the role of this homolog in mediating  $\text{Ca}^{2+}$  entry was not assessed in the current study [30]. Western blotting was performed 48 h post-transfection to validate the effectiveness of knockdown of protein expression. As shown in Fig. 4, Orai protein band densities were normalized to the  $\beta$ -actin loading control and expressed as a ratio. The Orai1 expression level in cells that were transfected with scrambled shRNA was determined to be  $1.21 \pm 0.21$  ratio units ( $n=4$ ). In contrast, when cells were transfected with Orai1 shRNA the ratio value was  $0.26 \pm 0.07$  ratio units ( $n=4$ ) and represented approximately 78% knockdown of Orai1. Expression of Orai3 was knocked down by 82% when compared to control cells that were transfected with scrambled shRNA. (The average ratio values of the Orai3 bands in cells transfected with scrambled and Orai3 shRNAs were  $1.95 \pm 0.29$  ( $n=4$ ) and  $0.35 \pm 0.10$  ratio units ( $n=4$ ), respectively). In addition, cell lysates from knocked down cells were probed for the expression of both Orai1 and Orai3 homologs to test for changes in the expression of the non-targeted homolog. In these experiments, the average Orai1 ratio value of expression in cells transfected with Orai3 shRNA was 1.07 ratio units ( $n=2$ ) and the ratio value of Orai3 expression in cells transfected with Orai1 shRNAs was 1.82 ratio units ( $n=2$ ). These values were comparable to control values and indicated there was no significant effect on the expression of the non-targeted homolog. An example of this control is shown in Additional file 2: Figure S2.

The functional consequences of knockdowns of Orai homologs on  $\text{Ca}^{2+}$  entry were investigated using live cell



$\text{Ca}^{2+}$  imaging methods. As shown in Fig. 5a, c, knockdown of Orai1 significantly attenuated the amplitude of SOCE in comparison with cells transfected with scrambled shRNA. While the mean SOCE amplitude for cells where Orai1 was knocked down was  $0.16 \pm 0.02$  ratio units ( $n=5$ ), the amplitude for cells transfected with scrambled shRNA was  $0.38 \pm 0.04$  ratio units ( $n=5$ ). However, knockdown of Orai3 did not significantly diminish the mean SOCE amplitude. In these cells, the peak amplitude of SOCE was on average  $0.27 \pm 0.01$  ratio units ( $n=5$ ). As shown in Fig. 5b, the genetic manipulation had no significant effect on the CPA-evoked  $\text{Ca}^{2+}$  release signal. The average amplitude of the CPA-evoked release signal in cells that were transfected with scrambled shRNA was  $0.16 \pm 0.02$  ratio units and that for cells transfected with Orai1 and Orai3 shRNAs were  $0.15 \pm 0.01$  and  $0.12 \pm 0.01$  ratio units, respectively.

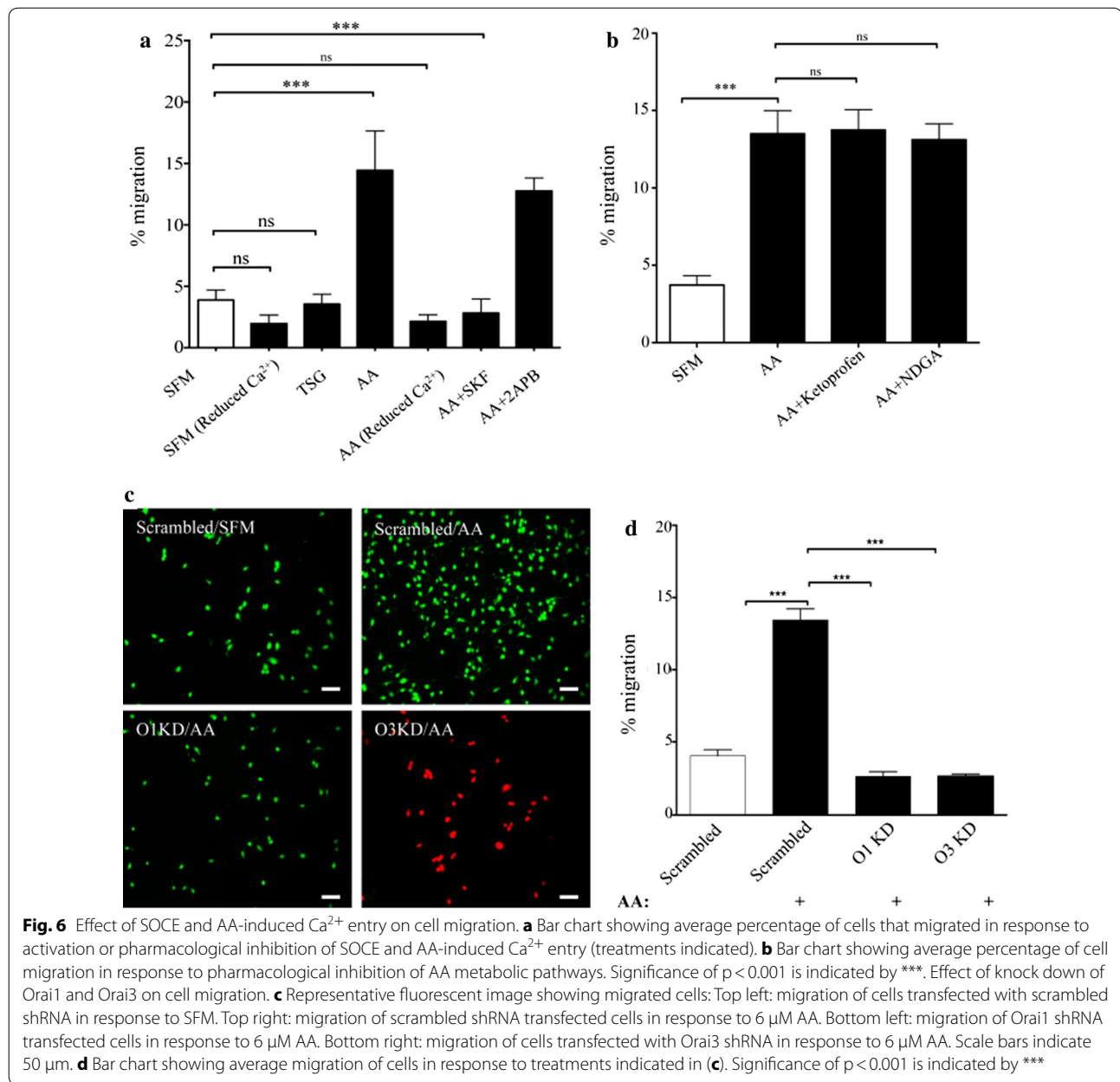


In contrast to the SOCE responses, knockdown of either Orai1 or Orai3 significantly decreased the amplitude of the AA-induced responses compared to cells transfected with scrambled shRNA. While the mean amplitude of the AA-induced  $\text{Ca}^{2+}$  entry in cells transfected with scrambled shRNA was  $1.68 \pm 0.32$  ratio units ( $n=5$ ), cells that were transfected with Orai1 or Orai3 shRNAs had significantly reduced peak amplitudes of  $0.29 \pm 0.09$  ( $n=6$ ) and  $0.29 \pm 0.10$  ( $n=6$ ) ratio units, respectively. These results indicated that both Orai1 as well as Orai3 were required for mediating  $\text{Ca}^{2+}$  entry in response to AA and that channels that contained predominantly Orai1 were required for SOCE.

#### Effects of AA-induced and store-operated $\text{Ca}^{2+}$ entry on cell migration

We next selectively activated store-operated or AA-induced  $\text{Ca}^{2+}$  entry to assess their relative effectiveness to induce migration in BON cells. We first tested whether the induced cell migration required extracellular  $\text{Ca}^{2+}$ . As shown in Fig. 6a, reduction of extracellular  $\text{Ca}^{2+}$  had minimal effect on the basal migration compared to SFM alone. For example, the percentage of cells migrated in SFM was  $3.89 \pm 0.40\%$  ( $n=4$ ) while the percentage of cells migrated in a reduced  $\text{Ca}^{2+}$ -containing SFM was  $1.96 \pm 0.40\%$  ( $n=3$ ). Moreover, direct activation of SOCE by treatment of BON cells with either  $1 \mu\text{M}$  TSG or  $30 \mu\text{M}$  CPA failed to enhance cell migration significantly





above basal levels with only  $3.54 \pm 0.47\%$  cells migrated ( $n = 3$ ). In contrast, migration of BON cells was enhanced approximately threefold in response to treatment with 6  $\mu$ M AA where  $14.43 \pm 1.61\%$  of cells migrated ( $n = 4$ ). Reducing extracellular Ca<sup>2+</sup> abrogated the AA-induced enhancement of cell migration ( $2.15 \pm 0.31\%$ ;  $n = 3$ ) consistent with a requirement for Ca<sup>2+</sup> entry. To further assess the relative contributions of store-operated- and AA-induced Ca<sup>2+</sup> entry in BON cell migration, the pharmacological inhibitors of SOCE, SKF and 2-APB, were tested on AA-induced BON cell migration. Treatment with SKF significantly reduced the AA-induced

cell migration. In these experiments only  $2.82 \pm 0.58\%$  cells on average migrated ( $n = 4$ ). In contrast, 2-APB had no significant effect on the AA-induced enhancement of cell migration when compared to AA alone. In these experiments  $12.76 \pm 0.53\%$  cells on average migrated ( $n = 4$ ). It was interesting to note that in contrast to the acute effects of AA-treatment where Ca<sup>2+</sup> entry was enhanced in the presence of 2-APB, inclusion of 2-APB did not enhance AA-induced cell migration. This most likely resulted from a difference in the time courses of treatment for Ca<sup>2+</sup> imaging and Boyden chamber experiments. Taken together, activation of AA-induced Ca<sup>2+</sup>

entry, but not SOCE, could mobilize a sub-population of BON cells to migrate in a Boyden chamber.

However, because AA can be readily metabolized into other bioactive classes of compounds such as leukotrienes and prostaglandins, we assessed whether AA-metabolites contributed in BON cell migration. Moreover reports by Mohamed Trebak's group demonstrated that leukotriene-C4 could mediate a store-independent  $\text{Ca}^{2+}$  entry via Orai1/3 channels [14, 24]. To test whether AA-metabolites were involved in BON cell migration, we treated the cells with pharmacological inhibitors of AA-metabolism. Ketoprofen, a non-selective inhibitor of cyclooxygenase I and II, and nordihydroguaiaretic acid (NDGA), a pan-lipoxygenase inhibitor were included along with AA in the migration assays. As shown in Fig. 6b, neither of these compounds caused a significant reduction in AA-induced cell migration. In presence of ketoprofen or NDGA,  $13.7 \pm 0.76\%$  ( $n=3$ ) or  $13.12 \pm 0.59\%$  ( $n=3$ ) cells migrated, respectively. These data were consistent with the idea that AA itself, and not its metabolite caused the enhancement of cell migration.

Because AA-induced  $\text{Ca}^{2+}$  entry is thought to be mediated by a channel that contains both Orai1 and Orai3, we investigated the role of these homologs in AA-induced cell migration. As shown in Fig. 7c, d, knockdown of either Orai1 or Orai3 in BON cells resulted in a dramatic reduction in AA-induced migration compared to cells transfected with scrambled shRNA. While  $13.45 \pm 0.77\%$  ( $n=3$ ) of the cells transfected with scrambled shRNA migrated when, only  $2.69 \pm 0.32\%$  ( $n=3$ ) of cells transfected with Orai1 shRNA and  $2.68 \pm 0.15\%$  ( $n=3$ ) of cells transfected with Orai3 shRNA migrated in response to application of  $6 \mu\text{M}$  AA. Since knocking down Orai3 had a minimal effect on SOCE, the result of this experiment was consistent with our pharmacological data that suggested that AA-induced  $\text{Ca}^{2+}$  entry is the dominant  $\text{Ca}^{2+}$  entry pathway regulating BON cell migration in vitro.

#### **Morphological and phenotypic changes following arachidonic acid treatment**

Transformed cells can exhibit a migratory phenotype that correlates with increased metastatic potential. In BON cells that express both epithelial and neuroendocrine features, this can be achieved via neuroendocrine-to-mesenchymal transition (NMT). This transition is characterized by a reduction in neuroendocrine markers and altered expression of mesenchymal proteins [32–34]. Thus, we assessed whether AA treatment could induce morphological changes and alter expression of markers of NMT including chromogranin A (CGA) E-cadherin,  $\alpha$ -smooth muscle actin ( $\alpha$ -SMA) and snail family transcriptional repressor 1 (Snail1).

In these experiments, cells were plated onto coverslips or applied to transwell inserts, serum starved for 4 h, incubated overnight or for up to 48 h in growth medium supplemented with  $6 \mu\text{M}$  arachidonic acid or 0.1% DMSO as vehicle control and subsequently assessed by immunofluorescence. Morphological changes induced by AA treatment were visualized by F-actin staining using fluorescently labeled phalloidin. The majority of control cells appeared clustered and were rounded or oblong in shape ( $\sim 97\%$ ), whereas the majority of AA treated cells ( $\sim 93\%$ ) exhibited an elongated, flattened shape that was often decorated with multiple cellular processes. Additional images of these morphologies are shown in Additional file 3: Figure S3. As indicated above, migration assays revealed that AA treatment induced migration in a subset of BON cells. Therefore, we removed and imaged chamber inserts following AA treatment and assessed the morphology of non-migrated and migrated cells using confocal microscopy. As shown in Fig. 7a, b, staining for F-actin revealed distinctive morphologies between these two populations. The unmigrated cells on the surface of the transwell insert appeared to be in clusters and exhibited rounded shapes whereas the migrated cells on the bottom of the insert typically exhibited flattened irregular shapes with processes. These respective morphologies were similar to those observed for cells cultured on glass coverslips that were treated with vehicle or AA.

One hallmark of NMT is a reduction in the neuroendocrine secretory granule protein CgA. Under our experimental conditions, approximately 34% of cells in control groups exhibited perinuclear and subplasmamembrane distribution of CgA signal. Following overnight AA treatment, less than 15% of cells showed labeling. Figure 7c, d indicated that following AA treatment there was about a 50% reduction in the number of cells expressing CgA. Moreover, the treated cells appeared much more mesenchymal in morphology and some cells showed persistent expression and ubiquitous distribution of the CgA label through out the cell including the filipodial extensions. Longer treatments (24–48 h) showed a further reduction in the number of CgA expressing cells.

Furthermore, as shown in Fig. 7e, f, there was a clear reduction in the intensity of E-cadherin staining following AA treatment. In comparing images of control and AA-treated cells, there was typically greater than 60% reduction in the mean pixel intensity of the E-cadherin (green) signal. The findings were consistent with NMT phenotype. Of note, the E-cadherin signal in BON cells had an atypical nuclear distribution, similar to that previously shown to correlate with invasiveness in pancreatic NETs [34].

In contrast, we did not observe changes in expression levels of the mesenchymal proteins  $\alpha$ -SMA and Snail1

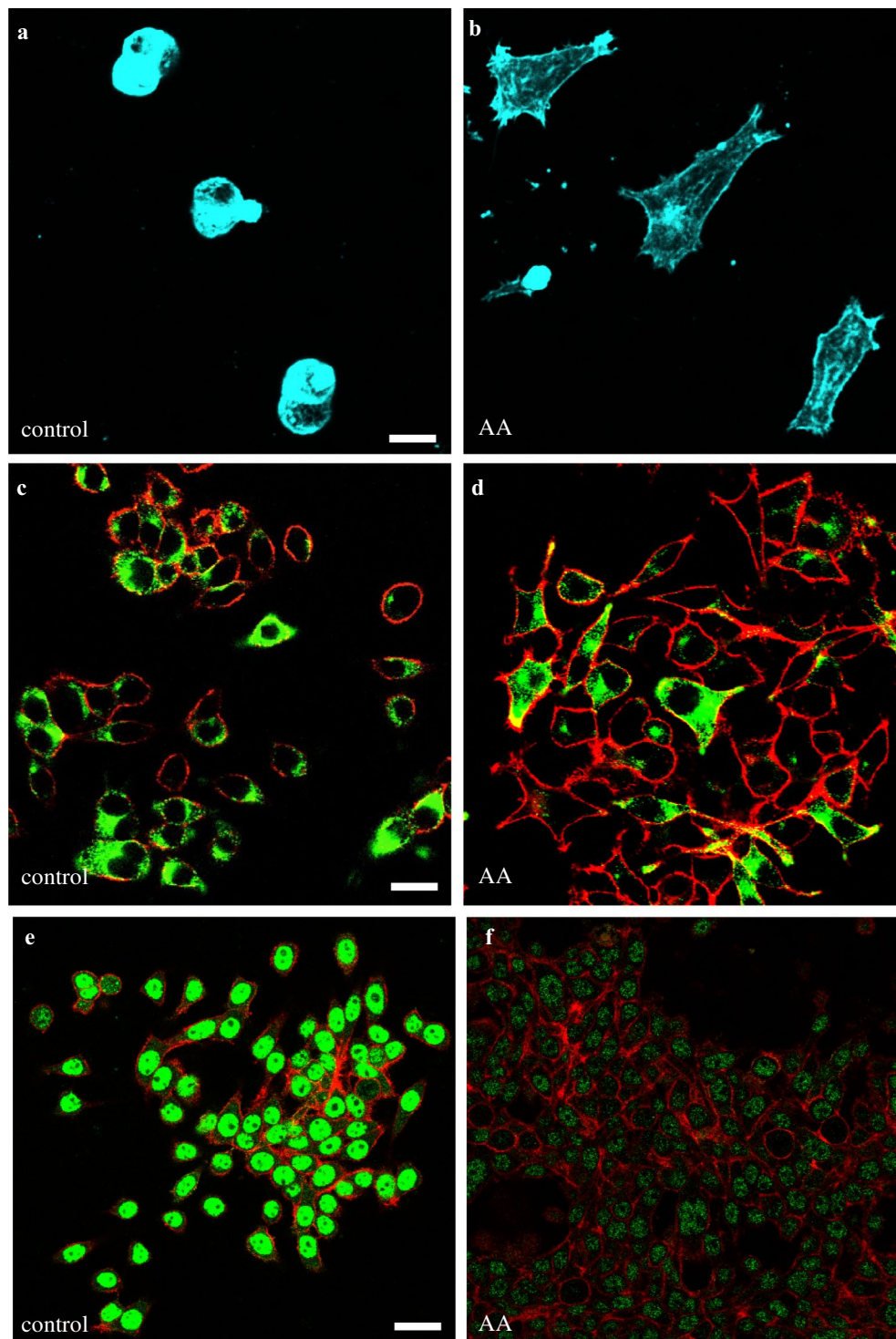


**Fig. 7** Morphological and phenotypic changes prior to or following AA treatment. **a, b** Confocal images of unimigrated and migrated BON cells acquired from transwell inserts following treatment with 6  $\mu$ M AA for 8 h. Cell morphology was visualized by F-actin labeling with Alexa Fluor 633 conjugated phallotoxin. **c, d** Images of BON cell cultures following overnight treatment with vehicle alone (**c**) or with (**d**) AA treatment. Cells were labeled with antisera for CgA (green) and AlexaFluor 546 conjugated phallotoxin for F-actin (red). Percentages of cells expressing CgA were quantified under the two treatment conditions. **e, f** Assessment of E-cadherin expression levels (green) and F-actin (red) following overnight treatment with vehicle or AA, respectively. Each image set was obtained with the same intensity and settings to assess relative changes in fluorescence intensity evoked by treatment. Scale bars on image sets were 15, 20 and 25  $\mu$ m, respectively

following AA treatment (data not shown). The lack of an effect may be in part explained by the surprising expression of these markers in BON cells prior to AA treatment.

## Discussion

Previous work from our laboratory provided molecular and functional characterization of the SOCE pathway [30] in a variety of GEPNET cell lines. It was revealed that BON cells robustly expressed messages for Orai1 and Orai3, but not Orai2. In the current study, we extended these observations to demonstrate protein expression and functional contributions of Orai1 and Orai3 channel subunits to  $Ca^{2+}$  signals and cell migration. These findings support the hypothesis that AA-induced  $Ca^{2+}$  entry through an Orai1/Orai3 containing channel was important for migration of a sub-population of BON cells.

Recent work from several groups has demonstrated a requirement of Orai1-containing channels for SOCE and cell migration in some tumor cell lines. Although knockdown of Orai1 suppressed BON cell migration, it was unlikely that the suppression was mediated by inhibition of a canonical store-operated channel. This idea was supported by the observation that direct activation of SOCE by TSG-induced store depletion was ineffective at stimulating migration. Although this finding is tempered by the caveat that prolonged treatment with TSG can induce ER stress and apoptosis.

Our contention is that it was more likely that the knockdown of Orai1 inhibited an AA-induced  $Ca^{2+}$  entry channel that contained Orai3 as well as Orai1 subunits. Consistent with this proposal, we found that treatment with AA resulted in  $Ca^{2+}$  influx that was distinct from canonical SOCE. Moreover, activation of this pathway stimulated migration of BON cells, and that when inhibited, abrogated the enhancement in migration. These data showed that Orai1 was necessary for mediating SOCE, whereas AA-induced  $Ca^{2+}$  entry as well as BON cell migration required both Orai1 and Orai3.

The AA-induced  $Ca^{2+}$  entry channel characterized here is reminiscent of the store-independent ARC channel described by Shuttleworth's group [35, 36]. More recently, Trebak's group identified an Orai1/Orai3-containing leukotriene-C4 (LTC4) inducible channel that mediated  $Ca^{2+}$  entry in vascular smooth muscle cells in response to thrombin stimulation [14]. Although we did not directly test whether LTC4 could activate  $Ca^{2+}$  entry or cell migration in our system, pharmacological inhibition of AA-metabolism did not suppress AA-induced cell migration. This indicated that the enhancement of cell migration observed was largely due to AA itself and not its metabolite.

Assessment of migration using pharmacological tools was also consistent with the involvement of an Orai3-containing channel. Typically, 2-APB has been used as a tool to block SOCE and has been shown in some studies to inhibit cell migration. For example, 2-APB was shown to block EGF-induced cell migration in nasopharyngeal carcinoma [21] and wound healing of clear cell renal cell carcinoma [20]. However, we found that treatment with 2-APB suppressed SOCE but not AA-induced  $Ca^{2+}$  entry or AA-evoked BON cell migration, consistent with previous work that showed 2-APB does not block, and may even enhance, conductance in Orai3-containing channels. In contrast, the broader spectrum channel blocker SKF effectively blocked  $Ca^{2+}$  entry through Orai1- and Orai3-containing channels. These findings indicated a novel mechanism by which Orai-mediated  $Ca^{2+}$  entry may contribute to migration in this biologically idiosyncratic group of cancers.

In this context, it should be noted that a mutual antagonism between SOCE- and AA-evoked  $Ca^{2+}$  entry has been observed in other cell types [37–39] and thus modes of entry may interact to set the migration potential of NET cells. Indeed, the migration potential may in part be mediated by NMT, consistent with our findings that AA treatment altered the morphology and phenotype of BON cells such that the migrated cells appeared more mesenchymal in state.

Based on our findings it is tempting to speculate that the AA-induced  $Ca^{2+}$  channel has relevance for GEPNET pathophysiology. For example, these cancers are thought to arise from neurosecretory cells in the gastrointestinal tract and commonly metastasize to the liver. Both the small intestine and liver exhibit elevated concentrations of AA [40, 41] compared to other regions of the gut. Moreover, neuroendocrine tumor cells are known to secrete several biogenic amines and peptides. Many of these secretory products have been linked with increased production of AA in different cell types. For example, serotonin has been shown to stimulate the  $PLA_2$ -driven synthesis of AA in hippocampal neurons [42]. Bradykinin, an intestinal peptide that is secreted by neuroendocrine cells has been shown to stimulate AA synthesis in gut [43]. Moreover, we recently reported that conditioned media (CM) derived from cultured BON cells had a pro-migratory effect on these tumor cells, presumably through an autocrine mechanism [31]. Although we did not directly test whether treatment with CM stimulated synthesis of AA in our system, unpublished experiments related to this study showed that the pharmacological inhibition of AA synthesis resulted in a decrease in CM-evoked cell migration that could be recovered by application of AA.

## Conclusions

The current manuscript demonstrates that treatment with AA induced  $\text{Ca}^{2+}$  entry through an Orai1/Orai3 heteromeric ion channel and that this mode of  $\text{Ca}^{2+}$  entry is important for migration in a GEPNET cell-line. The findings suggest that AA-induced  $\text{Ca}^{2+}$  entry may help set the migratory potential of these tumor cells and identify  $\text{Ca}^{2+}$  entry through the Orai3-containing channel as a novel signal for BON cell migration that may be exploited for therapeutic prevention of recurring GEPNET metastasis.

## Additional files

**Additional file 1: Figure S1.** Calcium entry amplitude and dynamics evoked by AA treatments. (A) Bar graph showing the peak amplitude increases in cytosolic  $\text{Ca}^{2+}$  in fura-2 loaded BON cells induced by application of different concentrations of arachidonic acid. Peak ratio changes for 1, 3, 6, 10 and 30  $\mu\text{M}$  AA applications was  $0.45 \pm 0.19$ ,  $0.69 \pm 0.24$ ,  $1.48 \pm 0.18$ ,  $2.10 \pm 0.27$  and  $4.71 \pm 0.72$ , respectively ( $n = 3$ ). B. Examples of typical  $\text{Ca}^{2+}$  dynamics induced by AA treatment. On restoration of extracellular  $\text{Ca}^{2+}$  we observed two typical responses: a more common, complex waveform (black) and a slower, gradual and sustained rise (red). Scale bars = 100 s and 0.500 ratio units.

**Additional file 2: Figure S2.** Selective knockdown of Orai channel subunit proteins. Western blot data demonstrating that silencing of one Orai channel paralog does not induce changes in expression of the other paralog. shRNAs are indicated as scrambled (Scr) or selective for Orai 1 (O1) or Orai 3 (O3). Actin expression was used as a loading control.

**Additional file 3: Figure S3.** Morphological changes induced in BON cells by overnight treatment with 6  $\mu\text{M}$  AA. Cell shapes were visualized by treatment with phalloxin fluorescently-labeled with Alexa Fluor 546 (red) or 633 (cyan). Confocal images of cells in culture are shown following treatment with vehicle contro (DMSO) or AA as indicated.

## Authors' contributions

PG designed experiments, acquired and analyzed data and wrote the manuscript. TP performed experiments and analyzed immunofluorescence data. DG conceived and directed the research, reviewed the data and wrote and edited the manuscript. All authors reviewed the manuscript. All authors read and approved the final manuscript.

## Acknowledgements

We thank Dr. Andrea Kalinoski and the Advanced Microscopy and Imaging Center at University of Toledo for assistance with the confocal microscopy.

## Competing interests

The authors declare that they have no competing interests.

## Availability of data and materials

The data used and/or analysed for the current study are available from the corresponding author on reasonable request.

## Consent for publication

Not applicable.

## Ethics approval and consent to participate

Not applicable.

## Funding

This study was supported by a grant from the Raymond and Beverly Sackler Foundation to DRG and University of Toledo Graduate Student Research award to PG.

## Publisher's Note

Springer Nature remains neutral with regard to jurisdictional claims in published maps and institutional affiliations.

Received: 31 October 2017 Accepted: 24 February 2018

Published online: 02 March 2018

## References

- Feske S, Gwack Y, Prakriya M, Srikanth S, Puppel SH, Tanasa B, Hogan PG, Lewis RS, Daly M, Rao A. A mutation in Orai1 causes immune deficiency by abrogating CRAC channel function. *Nature*. 2006;441(7090):179–85.
- Mercer JC, Dehaven WI, Smyth JT, Wedel B, Boyles RR, Bird GS, Putney JW Jr. Large store-operated calcium selective currents due to co-expression of Orai1 or Orai2 with the intracellular calcium sensor, Stim1. *J Biol Chem*. 2006;281(34):24979–90.
- Peinelt C, Vig M, Koomoa DL, Beck A, Nadler MJ, Koblan-Huberson M, Lis A, Fleig A, Penner R, Kinet JP. Amplification of CRAC current by STIM1 and CRACM1 (Orai1). *Nat Cell Biol*. 2006;8(7):771–3.
- Prakriya M, Feske S, Gwack Y, Srikanth S, Rao A, Hogan PG. Orai1 is an essential pore subunit of the CRAC channel. *Nature*. 2006;443(7108):230–3.
- Roos J, DiGregorio PJ, Yeromin AV, Ohlsen K, Lioudyno M, Zhang S, Safrina O, Kozak JA, Wagner SL, Cahalan MD, et al. STIM1, an essential and conserved component of store-operated  $\text{Ca}^{2+}$  channel function. *J Cell Biol*. 2005;169(3):435–45.
- Soboloff J, Spassova MA, Tang XD, Hewavitharana T, Xu W, Gill DL. Orai1 and STIM reconstitute store-operated calcium channel function. *J Biol Chem*. 2006;281(30):20661–5.
- Yeromin AV, Zhang SL, Jiang W, Yu Y, Safrina O, Cahalan MD. Molecular identification of the CRAC channel by altered ion selectivity in a mutant of Orai. *Nature*. 2006;443(7108):226–9.
- Liou J, Kim ML, Heo WD, Jones JT, Myers JW, Ferrell JE Jr, Meyer T. STIM is a  $\text{Ca}^{2+}$  sensor essential for  $\text{Ca}^{2+}$ -store-depletion-triggered  $\text{Ca}^{2+}$  influx. *Curr Biol CB*. 2005;15(13):1235–41.
- Shaw PJ, Feske S. Physiological and pathophysiological functions of SOCE in the immune system. *Front Biosci*. 2012;4:2253–68.
- Motiani RK, Stolwijk JA, Newton RL, Zhang X, Trebak M. Emerging roles of Orai3 in pathophysiology. *Channels*. 2013;7(5):392–401.
- Dubois C, Vanden Abeele F, Lehen'kyi V, Gkika D, Guarmit B, Lepage G, Slomianny C, Borowiec AS, Bidaux G, Benahmed M, et al. Remodeling of channel-forming ORAI proteins determines an oncogenic switch in prostate cancer. *Cancer Cell*. 2014;26(1):19–32.
- Yang S, Zhang JJ, Huang XY. Orai1 and STIM1 are critical for breast tumor cell migration and metastasis. *Cancer Cell*. 2009;15(2):124–34.
- Bisaillon JM, Motiani RK, Gonzalez-Cobos JC, Potier M, Halligan KE, Alzawahra WF, Barroso M, Singer HA, Jourde'heuil D, Trebak M. Essential role for STIM1/Orai1-mediated calcium influx in PDGF-induced smooth muscle migration. *Am J Physiol Cell Physiol*. 2010;298(5):C993–1005.
- Gonzalez-Cobos JC, Zhang X, Zhang W, Ruhle B, Motiani RK, Schindl R, Muik M, Spinelli AM, Bisaillon JM, Shinde AV, et al. Store-independent Orai1/3 channels activated by intracrine leukotriene C4: role in neointimal hyperplasia. *Circ Res*. 2013;112(7):1013–25.
- Chen YF, Chiu WT, Chen YT, Lin PY, Huang HJ, Chou CY, Chang HC, Tang MJ, Shen MR. Calcium store sensor stromal-interaction molecule 1-dependent signaling plays an important role in cervical cancer growth, migration, and angiogenesis. *Proc Natl Acad Sci USA*. 2011;108(37):15225–30.
- Schafer C, Rymarczyk G, Ding L, Kirber MT, Bolotina VM. Role of molecular determinants of store-operated  $\text{Ca}^{2+}$  entry (Orai1, phospholipase A2 group 6, and STIM1) in focal adhesion formation and cell migration. *J Biol Chem*. 2012;287(48):40745–57.
- Yang N, Tang Y, Wang F, Zhang H, Xu D, Shen Y, Sun S, Yang G. Blockade of store-operated  $\text{Ca}^{2+}$  entry inhibits hepatocarcinoma cell migration and invasion by regulating focal adhesion turnover. *Cancer Lett*. 2013;330(2):163–9.
- Umamura M, Baljinnnyam E, Feske S, De Lorenzo MS, Xie LH, Feng X, Oda K, Makino A, Fujita T, Yokoyama U, et al. Store-operated  $\text{Ca}^{2+}$  entry

- (SOCE) regulates melanoma proliferation and cell migration. *PLoS ONE*. 2014;9(2):e89292.
19. Zhu M, Chen L, Zhao P, Zhou H, Zhang C, Yu S, Lin Y, Yang X. Store-operated  $Ca^{2+}$  entry regulates glioma cell migration and invasion via modulation of Pyk2 phosphorylation. *J Exp Clin Cancer Res CR*. 2014;33(1):98.
  20. Kim JH, Lkhagvadorj S, Lee MR, Hwang KH, Chung HC, Jung JH, Cha SK, Eom M. Orai1 and STIM1 are critical for cell migration and proliferation of clear cell renal cell carcinoma. *Biochem Biophys Res Commun*. 2014;448(1):76–82.
  21. Zhang J, Wei J, Kanada M, Yan L, Zhang Z, Watanabe H, Terakawa S. Inhibition of store-operated  $Ca^{2+}$  entry suppresses EGF-induced migration and eliminates extravasation from vasculature in nasopharyngeal carcinoma cell. *Cancer Lett*. 2013;336(2):390–7.
  22. Chen YF, Chen YT, Chiu WT, Shen MR. Remodeling of calcium signaling in tumor progression. *J Biomed Sci*. 2013;20:23.
  23. Mignen O, Shuttleworth TJ. I(Arc), a novel arachidonate-regulated, noncapacitative  $Ca^{2+}$  entry channel. *J Biol Chem*. 2000;275(13):9114–9.
  24. Zhang W, Zhang X, Gonzalez-Cobos JC, Stolwijk JA, Matrougui K, Trebak M. Leukotriene-C4 synthase, a critical enzyme in the activation of store-independent Orai1/Orai3 channels, is required for neointimal hyperplasia. *J Biol Chem*. 2015;290(8):5015–27.
  25. Mignen O, Thompson JL, Shuttleworth TJ. Both Orai1 and Orai3 are essential components of the arachidonate-regulated  $Ca^{2+}$ -selective (ARC) channels. *J Physiol*. 2008;586(1):185–95.
  26. Navarro-Tito N, Robledo T, Salazar EP. Arachidonic acid promotes FAK activation and migration in MDA-MB-231 breast cancer cells. *Exp Cell Res*. 2008;314(18):3340–55.
  27. Kim JI, Lakshmikanthan V, Frilot N, Daaka Y. Prostaglandin E2 promotes lung cancer cell migration via EP4-betaArrestin1-c-Src signalsome. *Mol Cancer Res MCR*. 2010;8(4):569–77.
  28. Moraes J, Assreuy J, Canetti C, Barja-Fidalgo C. Leukotriene B4 mediates vascular smooth muscle cell migration through alpha5beta3 integrin transactivation. *Atherosclerosis*. 2010;212(2):406–13.
  29. Martinez-Orozco R, Navarro-Tito N, Soto-Guzman A, Castro-Sanchez L, Perez Salazar E. Arachidonic acid promotes epithelial-to-mesenchymal-like transition in mammary epithelial cells MCF10A. *Eur J Cell Biol*. 2010;89(6):476–88.
  30. Arunachalam S, Zhelay T, Giovannucci DR. Molecular and functional characterization of non voltage-operated  $Ca^{2+}$  entry in gastrointestinal neuroendocrine tumor cells. *Int J Physiol Pathophysiol Pharmacol*. 2010;2(2):125–36.
  31. Goswamee P, Arunachalam S, Mehta S, Nasim R, Gunning WT, Giovannucci DR. Gastro-enteropancreatic neuroendocrine tumor cell dynamics in liver microvasculature. *Microsc Microanal*. 2015;21(3):655–65.
  32. Abbracchio MP, Burnstock G, Verkhratsky A, Zimmermann H. Purinergic signalling in the nervous system: an overview. *Trends Neurosci*. 2009;32(1):19–29.
  33. Leu FP, Nandi M, Niu C. The effect of transforming growth factor beta on human neuroendocrine tumor BON cell proliferation and differentiation is mediated through somatostatin signaling. *Mol Cancer Res MCR*. 2008;6(6):1029–42.
  34. Yonemori K, Kurahara H, Maemura K, Mataka Y, Sakoda M, Iino S, Ueno S, Shinchi H, Natsugoe S. Impact of snail and E-cadherin expression in pancreatic neuroendocrine tumors. *Oncol Lett*. 2017;14(2):1697–702.
  35. Holmes AM, Roderick HL, McDonald F, Bootman MD. Interaction between store-operated and arachidonate-activated calcium entry. *Cell Calcium*. 2007;41(1):1–12.
  36. Mignen O, Thompson JL, Shuttleworth TJ. The molecular architecture of the arachidonate-regulated  $Ca^{2+}$ -selective ARC channel is a pentameric assembly of Orai1 and Orai3 subunits. *J Physiol*. 2009;587(Pt 17):4181–97.
  37. Mignen O, Thompson JL, Shuttleworth TJ. Reciprocal regulation of capacitative and arachidonate-regulated noncapacitative  $Ca^{2+}$  entry pathways. *J Biol Chem*. 2001;276(38):35676–83.
  38. Moneer Z, Taylor CW. Reciprocal regulation of capacitative and non-capacitative  $Ca^{2+}$  entry in A7r5 vascular smooth muscle cells: only the latter operates during receptor activation. *Biochem J*. 2002;362(Pt 1):13–21.
  39. Luo D, Broad LM, Bird GS, Putney JW Jr. Mutual antagonism of calcium entry by capacitative and arachidonic acid-mediated calcium entry pathways. *J Biol Chem*. 2001;276(23):20186–9.
  40. Capdevila J, Chacos N, Werringloer J, Prough RA, Estabrook RW. Liver microsomal cytochrome P-450 and the oxidative metabolism of arachidonic acid. *Proc Natl Acad Sci USA*. 1981;78(9):5362–6.
  41. Eberhart CE, Dubois RN. Eicosanoids and the gastrointestinal tract. *Gastroenterology*. 1995;109(1):285–301.
  42. Felder CC, Kanterman RY, Ma AL, Axelrod J. Serotonin stimulates phospholipase A2 and the release of arachidonic acid in hippocampal neurons by a type 2 serotonin receptor that is independent of inositol phospholipid hydrolysis. *Proc Natl Acad Sci USA*. 1990;87(6):2187–91.
  43. Lawson LD, Powell DW. Bradykinin-stimulated eicosanoid synthesis and secretion by rabbit ileal components. *Am J Physiol*. 1987;252(6 Pt 1):G783–90.

Submit your next manuscript to BioMed Central and we will help you at every step:

- We accept pre-submission inquiries
- Our selector tool helps you to find the most relevant journal
- We provide round the clock customer support
- Convenient online submission
- Thorough peer review
- Inclusion in PubMed and all major indexing services
- Maximum visibility for your research

Submit your manuscript at  
[www.biomedcentral.com/submit](http://www.biomedcentral.com/submit)

